FFT-Spread Faster-Than-Nyquist Signaling in Frequency-Selective Fading Channel

Takumi Ishihara and Shinya Sugiura*
Institute of Industrial Science, The University of Tokyo
Meguro-Ku, Tokyo 153-8505, Japan
Email: {t.ishihara@ieee.org, sugiura@iis.u-tokyo.ac.jp}

***Abstract*—In this paper, we propose novel reduced-complexity fast Fourier transform (FFT)-spread faster-than-Nyquist (FTN) signaling with optimal power allocation for a frequency-selective fading channel. The information rate of the proposed FTN signaling is approximately derived by relying on the circulant approximation of the FTN-specific intersymbol interference matrix and noise covariance matrix. This allows us to constitute efficient calculations of precoding and weighting matrices. The power allocation coefficients are optimized such that the approximated information rate is maximized. Our simulation results demonstrate that the proposed scheme achieves the bit error ratio performance close to the conventional eigenvalue-decomposition (EVD)-precoded FTN signaling counterpart that is optimal in terms of an achievable information rate while significantly reducing the computational complexity as low as the order of $\mathcal{O}(N \log N)$.**

I. Introduction

Conventional wireless communication systems are designed based on the Nyquist criterion, which defines a minimum symbol interval by $T_0 = 1/(2W)$, where $2W$ represents the bandwidth of an ideal rectangular shaping filter, and the associated maximum symbol rate is $1/T_0$. The excess bandwidth of $2W(1+\beta)$ is induced when employing a realistic root raised cosine (RRC) shaping filter having a roll-off factor $\beta > 0$. Hence, the achievable spectral efficiency of Nyquist signaling based on an RRC shaping filter becomes $(1+\beta)$-times lower than that of an idealistic rectangular shaping filter ($\beta = 0$). To overcome this limitation, the concept of faster-than-Nyquist (FTN) signaling has been explored for more than 50 years [1–3]. In FTN signaling, a symbol interval is set lower than that of Nyquist signaling, i.e., $T = \tau T_0$, where τ $(0 < \tau \leq 1)$ represents a symbol packing ratio, hence achieving a higher symbol rate than the Nyquist signaling counterpart, which is, naturally, achieved at the cost of the detrimental intersymbol interference (ISI) effects.

To efficiently demodulate ISI-contaminated FTN symbols, several time-domain (TD) receivers have been developed [4–7]. In [4], the TD trellis-based iterative decoding algorithm was first developed. In [5], the TD equalizer based on the Bahl, Cocke, Jelinek, and Raviv (BCJR) algorithm was presented. Also, Prlja *et al.* in [6] conceived the reduced-state M-algorithm-based BCJR (M-BCJR) algorithm to further reduce the decoding complexity. Moreover, in [7], the modified M-BCJR algorithm was proposed for the sake of striking a flexible balance between the detection performance and complexity. However, the computational complexity of TD trellis-based detectors significantly increases upon increasing the effective tap length and the constellation size, which becomes prohibitively high, especially in a realistic frequency-selective fading channel.

By contrast, low-complexity frequency-domain (FD) FTN receivers have been developed [8–10]. In [8], the single-carrier FD equalization (FDE) algorithm with the aid of cyclic prefix (CP) was first applied to FTN signaling, where the FD weights were derived based on the minimum-mean-square-error (MMSE) criterion. Owing to the efficient fast Fourier transform (FFT)-based implementation, practical low-complexity detection was achieved even in a highly dispersive frequency-selective fading channel. Moreover, in [9], the hard-decision MMSE-FDE algorithm in [8] was extended to its soft-decision (SoD) counterpart to support iterative detection. In [10], the low-complexity FDE algorithm, capable of joint channel estimation and data detection, was presented for FTN signaling in a frequency-selective fading channel.

Precoded FTN signaling relying on the matrix factorization was proposed [11–14]. In [11], the capacity of FTN signaling was derived based on the eigenvalue decomposition (EVD) of an FTN-induced ISI matrix, showing that the capacity of EVD-precoded FTN signaling without power allocation is identical to that of unprecoded FTN signaling in [15]. Furthermore, optimal power allocation was introduced to EVD-precoded FTN signaling [12, 16], which achieves a higher capacity than unprecoded FTN signaling and classic Nyquist signaling when employing the RRC shaping filter having $\beta > 0$ for each scheme [3, 14, 16]. Also, the capacity of EVD-precoded FTN signaling with optimal power allocation is maximized when $\tau = 1/(1+\beta)$, which achieves the spectral efficiency equal to that of Nyquist signaling employing an idealistic rectangular shaping filter ($\beta = 0$) [3, 14, 16]. Note that optimal power allocation of EVD-precoded FTN signaling [12] is implementable without elaborate symbol truncation only for $1/(1+\beta) \leq \tau \leq$

Postprint accepted on 19 Jan. 2022 for publication in *IEEE International Conference on Communications (ICC)*, 2022.

1 [3, 14, 16]. Furthermore, in [14], EVD-precoded FTN signaling with optimal power allocation designed for an AWGN channel [12] was extended to that supporting a frequency-selective fading channel, and the associated information rate was derived. However, the computational complexity of the EVD-precoded FTN signaling scheme [14] is as prohibitively high as $\mathcal{O}(N^3)$ per block transmission.

The novel contribution of this paper is that we propose novel reduced-complexity FFT-spread FTN signaling with optimal power allocation for a frequency-selective fading channel. Owing to the low-complexity FFT-based implementation, the computational complexity order of the proposed FTN transmitter and receiver is as low as $\mathcal{O}(N \log_2 N)$ per block. More specifically, the ISI matrix and the correlated noise covariance matrix, which are specific to received FTN signals, are approximated by circulant matrices. This allows us to decompose the received FTN signal into N independent parallel substreams with the aid of FFT-based factorization, hence enabling simplified symbol-by-symbol demodulation. In our simulations, it is demonstrated that the proposed scheme achieves the BER performance close to that of the conventional EVD-precoded FTN signaling counterpart [14], which is highly complex but optimal in terms of an information rate.

II. Proposed Reduced-Complexity FFT-spread FTN Signaling with Optimal Power Allocation

In this section, we propose novel reduced-complexity FFT-spread FTN signaling with optimal power allocation for a frequency-selective fading channel. The block diagram of the proposed FTN system is shown in Fig. 1. At the transmitter, information bits are modulated onto N-length complex-valued symbols $\mathbf{s} = [s_0, \cdots, s_{N-1}]^T \in \mathbb{C}^N$, where $\mathbb{E}[|s_k|^2] = \sigma_{\rm s}^2$ $(k = 0, \cdots, N-1)$, and $\mathbb{E}[\cdot]$ is the expectation operation. Similar to conventional FTN signaling of [8, 10], the 2ν-length CP symbols are added to the precoded symbols $\mathbf{x}$ as follows:

$$\begin{aligned} \mathbf{x}_{\rm cp} &= [x_{{\rm cp},0}, \cdots, x_{{\rm cp},N+2\nu-1}] \in \mathbb{C}^{N+2\nu} && (1)\\ &= \mathbf{A}_{\rm cp}\mathbf{x} && (2)\\ &= \mathbf{A}_{\rm cp}\mathbf{P}\mathbf{s}, && (3)\end{aligned}$$

where

$$\mathbf{A}_{\rm cp} = \begin{bmatrix} \mathbf{0}_{2\nu\times(N-2\nu)} & \mathbf{I}_{2\nu} \\ & \mathbf{I}_N \end{bmatrix} \in \mathbb{R}^{(N+2\nu)\times N}, \quad (4)$$

and $\mathbf{0}_{2\nu\times(N-2\nu)}$ denotes the $(2\nu\times(N-2\nu))$-sized zero matrix. Furthermore, $\mathbf{P} \in \mathbb{C}^{N\times N}$ is a precoding matrix. The CP-added FTN signal $x_{\rm cp}(t)$ is given by

$$x_{\rm cp}(t) = \sum_n x_{{\rm cp},n} h(t - nT), \quad (5)$$

At the receiver, the received signal after matched-filtering is represented by

$$y_{\rm cp}(t) = \sum_{l=0}^{L-1} \sum_n h_l x_{{\rm cp},n} g(t - (l+n)T) + \eta(t), \quad (6)$$

By removing the 2ν samples associated with CP from the received sample block $\mathbf{y} = [y_{\rm cp}(0), y_{\rm cp}(T), \cdots, y_{\rm cp}(N+2\nu-1)]^T$, the N-length received block are obtained as

$$\begin{aligned} \mathbf{r} &= [r_0, \cdots, r_{N-1}]^T \in \mathbb{C}^N && (7)\\ &= [y_{\rm cp}(\nu T), \cdots, y_{\rm cp}((N+\nu-1)T)]^T && (8)\\ &= \mathbf{R}_{\rm cp}\mathbf{G}_{{\rm h},N+2\nu}\mathbf{A}_{\rm cp}\mathbf{x} + \boldsymbol{\eta}, && (9)\end{aligned}$$

where

$$\mathbf{R}_{\rm cp} = [\mathbf{0}_{N\times\nu} \ \ \mathbf{I}_N \ \ \mathbf{0}_{N\times\nu}] \in \mathbb{R}^{N\times(N+2\nu)}, \quad (10)$$

while $\mathbf{G}_{{\rm h},N+2\nu}$ is the $((N+2\nu)\times(N+2\nu))$-sized ISI matrix whose kth-row and mth column entry is given by

$$\mathbf{G}_{\rm h}(k,m) = \sum_{l=0}^{L-1} h_l g(kT - (m+l)T). \quad (11)$$

Furthermore, by assuming the condition of

$$g(kT) = 0 \quad \text{for } |k| > \nu, \quad (12)$$

(9) is approximated by [8–10]

$$\mathbf{r} \simeq \mathbf{G}_{\rm c}\mathbf{x} + \boldsymbol{\eta}, \quad (13)$$

where the matrix $\mathbf{G}_{\rm c} \in \mathbb{C}^{N\times N}$ is the circulant matrix whose EVD is given by

$$\mathbf{G}_{\rm c} = \mathbf{Q}^H \boldsymbol{\Theta} \mathbf{Q}. \quad (14)$$

Furthermore, $\mathbf{Q} \in \mathbb{C}^{N\times N}$ in (14) represents the normalized discrete Fourier transform (DFT) matrix whose kth-row and mth-column entry is given by $(1/\sqrt{N})\exp[-2\pi j(k-1)(m-1)/N]$. Additionally, $\boldsymbol{\Theta} = {\rm diag}\{\theta_0, \cdots, \theta_{N-1}\}$ is a diagonal matrix having the diagonal elements calculated by the FFT of the first column of $\mathbf{G}_{\rm c}$ [8, 10].

A. Approximated Mutual Information

Mutual information between the received block $\mathbf{r}$ and the transmit symbols $\mathbf{x}$ is formulated by

$$\begin{aligned} I(\mathbf{x};\mathbf{r}) &= h_{\rm e}(\mathbf{r}) - h_{\rm e}(\mathbf{r}|\mathbf{x}) && (15)\\ &= h_{\rm e}(\mathbf{r}) - h_{\rm e}(\boldsymbol{\eta}), && (16)\end{aligned}$$

where $h_{\rm e}(\cdot)$ represents a differential entropy. The upper bounds of the differential entropies of $\mathbf{r}$ and $\boldsymbol{\eta}$ are given by [17]

$$\begin{aligned} h_{\rm e}(\mathbf{r}) &\le \log_2\left((\pi e)^N \left|\mathbb{E}[\mathbf{r}\mathbf{r}^H]\right|_{\rm det}\right) && (17)\\ h_{\rm e}(\boldsymbol{\eta}) &\le \log_2\left((\pi e)^N \left|\mathbb{E}[\boldsymbol{\eta}\boldsymbol{\eta}^H]\right|_{\rm det}\right), && (18)\end{aligned}$$

where $|\cdot|_{\rm det}$ denotes the determinant operation. For an instantaneous fading channel, the covariance matrix of the received block is approximately given by

$$\begin{aligned} \mathbb{E}[\mathbf{r}\mathbf{r}^H] &\simeq \mathbb{E}[(\mathbf{G}_{\rm c}\mathbf{x} + \boldsymbol{\eta})(\mathbf{G}_{\rm c}\mathbf{x} + \boldsymbol{\eta})^H] && (19)\\ &= \mathbf{G}_{\rm c}\mathbb{E}[\mathbf{x}\mathbf{x}^H]\mathbf{G}_{\rm c}^H + \mathbb{E}[\boldsymbol{\eta}\boldsymbol{\eta}^H] && (20)\\ &= \mathbf{G}_{\rm c}\mathbf{R}_x\mathbf{G}_{\rm c}^H + N_0\mathbf{G}, && (21)\end{aligned}$$

where we have $\mathbf{R}_x = \mathbb{E}[\mathbf{x}\mathbf{x}^H]$.

As shown in [18], for the limit of $N \to \infty$, a banded

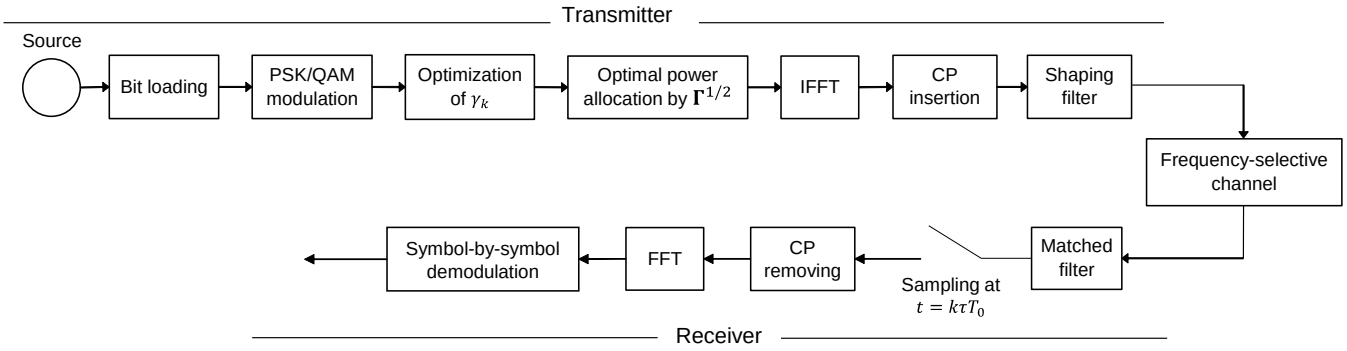

Fig. 1. System model of the proposed reduced-complexity FFT-spread FTN signaling scheme with optimal power allocation for a channel-uncoded scenario.

Toeplitz matrix $\mathbf{T} \in \mathbb{C}^{N\times N}$, whose first column and first row are given by $[t_0, t_1, \cdots, t_m, 0, \cdots, 0]^T$ and $[t_0, t_{-1}, \cdots, t_{-m}, 0, \cdots, 0]$, respectively, is asymptotically equivalent to a circulant matrix $\mathbf{C} \in \mathbb{C}^{N\times N}$, having the first column of $[t_0, t_1, \cdots, t_m, 0, \cdots, 0, t_{-m}, \cdots, t_{-1}]^T$. Hence, by assuming sufficiently large N and (12), the noise matrix $\mathbf{G}$, having the Toeplitz structure, is approximated by a circulant matrix whose first column is given by $\mathbf{g} = [g(0), g(T), \cdots, g(mT), 0, \cdots, 0, g(-mT), \cdots, g(-T)]^T$ $(0 \le m \le \lceil N/2 - 1 \rceil)$. In this paper, we assume the relationship of $m = \lceil N/2 - 1 \rceil$. This allows us to factorize $\mathbf{G}$ based on the FFT as follows:

$$\mathbf{G} \simeq \mathbf{Q}^H \mathbf{\Psi} \mathbf{Q}, \tag{22}$$

where we have $\mathbf{\Psi} = \mathrm{diag}[\psi_0, \cdots, \psi_{N-1}] \in \mathbb{R}^{N\times N}$, whose diagonal entries are given by the FFT of $\mathbf{g}$.

Under the assumption of $1/(1+\beta) < \tau \le 1$, the upper bound of mutual information $I(\mathbf{x};\mathbf{r})$ is approximated by

$$\begin{aligned}
I(\mathbf{x};\mathbf{r}) &\le \log_2 \frac{(\pi e)^N \left|\mathbb{E}[\mathbf{r}\mathbf{r}^H]\right|_{\det}}{(\pi e)^N \left|\mathbb{E}[\boldsymbol{\eta}\boldsymbol{\eta}^H]\right|_{\det}} && (23)\\
&\simeq \log_2 \frac{\left|\mathbf{G}_{\mathrm{c}}\mathbf{R}_x\mathbf{G}_{\mathrm{c}}^H + N_0\mathbf{G}\right|_{\det}}{\left|N_0\mathbf{G}\right|_{\det}} && (24)\\
&= \log_2 \left|\mathbf{I}_N + \frac{1}{N_0}\mathbf{G}_{\mathrm{c}}\mathbf{R}_x\mathbf{G}_{\mathrm{c}}^H\mathbf{G}^{-1}\right|_{\det} && (25)\\
&\simeq \log_2 \left|\mathbf{I}_N + \frac{1}{N_0}\mathbf{G}_{\mathrm{c}}\mathbf{R}_x\mathbf{G}_{\mathrm{c}}^H\mathbf{Q}^H\mathbf{\Psi}^{-1}\mathbf{Q}\right|_{\det} && (26)\\
&= \log_2 \left|\mathbf{I}_N + \frac{1}{N_0}\mathbf{Q}^H\mathbf{\Theta}\mathbf{Q}\mathbf{R}_x\mathbf{Q}^H\mathbf{\Theta}^H\mathbf{\Psi}^{-1}\mathbf{Q}\right|_{\det} && (27)\\
&= \log_2 \left|\mathbf{I}_N + \frac{1}{N_0}\mathbf{\Psi}^{-\frac{1}{2}}\mathbf{\Theta}\mathbf{Q}\mathbf{R}_x\mathbf{Q}^H\mathbf{\Theta}^H\mathbf{\Psi}^{-\frac{1}{2}}\right|_{\det}, && (28)
\end{aligned}$$

where the relationships of $|\mathbf{A}|_{\det}^{-1} = |\mathbf{A}^{-1}|_{\det}$ and $|\mathbf{I}_N + \mathbf{A}\mathbf{B}|_{\det} = |\mathbf{I}_N + \mathbf{B}\mathbf{A}|_{\det}$ are exploited.

Then, according to Hadamard's inequality [17, 19], the upper bound of the approximated mutual information (28) is maximized when $\mathbf{\Psi}^{-\frac{1}{2}}\mathbf{\Theta}\mathbf{Q}\mathbf{R}_x\mathbf{Q}^H\mathbf{\Theta}^H\mathbf{\Psi}^{-\frac{1}{2}}$ is a diagonal matrix, i.e., when $\mathbf{Q}\mathbf{R}_x\mathbf{Q}^H$ is a diagonal matrix. By letting $\mathbf{\Gamma} = \mathrm{diag}[\gamma_0, \cdots, \gamma_{N-1}] \in \mathbb{R}^{N\times N}$ be a real-valued diagonal matrix, (28) is maximized when the following equality holds:

$$\begin{aligned}
\mathbf{Q}\mathbf{R}_x\mathbf{Q}^H &= \sigma_{\mathrm{s}}^2\mathbf{\Gamma} && (29)\\
\mathbf{R}_x &= \sigma_{\mathrm{s}}^2\mathbf{Q}^H\mathbf{\Gamma}\mathbf{Q} && (30)\\
&\Leftrightarrow \mathbf{x} = \mathbf{Q}^H\mathbf{\Gamma}^{\frac{1}{2}}\mathbf{s}, && (31)
\end{aligned}$$

where we assume $\mathbb{E}[\mathbf{s}\mathbf{s}^H] = \sigma_{\mathrm{s}}^2\mathbf{I}_N$. Hence, the precoding matrix to be optimized is rewritten by

$$\mathbf{P} = \mathbf{Q}^H\mathbf{\Gamma}^{\frac{1}{2}} \tag{32}$$

By substituting (31) into (28), the upper bound of the approximated mutual information is maximized as follows:

$$\begin{aligned}
I(\mathbf{x};\mathbf{y}) &\le \log_2 \left|\mathbf{I}_N + \frac{\sigma_{\mathrm{s}}^2}{N_0}\mathbf{\Psi}^{-\frac{1}{2}}\mathbf{\Theta}\mathbf{\Gamma}\mathbf{\Theta}^H\mathbf{\Psi}^{-\frac{1}{2}}\right|_{\det} && (33)\\
&= \sum_{k=0}^{N-1} \log_2\left(1 + \frac{\sigma_{\mathrm{s}}^2}{N_0}\gamma_k\theta_k^2\psi_k^{-1}\right). && (34)
\end{aligned}$$

B. Optimal Power Allocation

The coefficients γ_k are optimized to maximize the r.h.s of (34) based on the Lagrange multiplier method. The transmit energy of the CP-added symbols $\mathbf{x}_{\mathrm{cp}} = \mathbf{A}_{\mathrm{cp}}\mathbf{Q}^H\mathbf{\Gamma}^{\frac{1}{2}}\mathbf{s}$ is calculated by [14]

$$\begin{aligned}
E &= \mathbb{E}\left[\mathbf{x}_{\mathrm{cp}}^H\mathbf{G}_{N+2\nu}\mathbf{x}_{\mathrm{cp}}\right] && (35)\\
&= \mathbb{E}[\mathrm{tr}\{\mathbf{x}_{\mathrm{cp}}^H\mathbf{G}_{N+2\nu}\mathbf{x}_{\mathrm{cp}}\}] && (36)\\
&= \mathbb{E}[\mathrm{tr}\{\mathbf{G}_{N+2\nu}\mathbf{x}_{\mathrm{cp}}\mathbf{x}_{\mathrm{cp}}^H\}] && (37)\\
&= \mathrm{tr}\{\mathbf{G}_{N+2\nu}\mathbf{A}_{\mathrm{cp}}\mathbf{Q}^H\mathbf{\Gamma}^{\frac{1}{2}}\mathbb{E}[\mathbf{s}\mathbf{s}^H]\mathbf{\Gamma}^{\frac{1}{2}}\mathbf{Q}\mathbf{A}_{\mathrm{cp}}^T\} && (38)\\
&= \sigma_{\mathrm{s}}^2\mathrm{tr}\{\mathbf{G}_{N+2\nu}\mathbf{A}_{\mathrm{cp}}\mathbf{Q}^H\mathbf{\Gamma}\mathbf{Q}\mathbf{A}_{\mathrm{cp}}^T\} && (39)\\
&= \sigma_{\mathrm{s}}^2\mathrm{tr}\{\mathbf{\Gamma}\mathbf{Q}\mathbf{A}_{\mathrm{cp}}^T\mathbf{G}_{N+2\nu}\mathbf{A}_{\mathrm{cp}}\mathbf{Q}^H\} && (40)\\
&= \sigma_{\mathrm{s}}^2\mathrm{tr}\{\mathbf{\Gamma}\mathbf{\Phi}\} && (41)\\
&= \sigma_{\mathrm{s}}^2\sum_{k=0}^{N-1}\gamma_k\phi_k, && (42)
\end{aligned}$$

where

$$\mathbf{\Phi} = \mathbf{Q}\mathbf{A}_{\mathrm{cp}}^T\mathbf{G}_{N+2\nu}\mathbf{A}_{\mathrm{cp}}\mathbf{Q}^H, \tag{43}$$

and $\mathbf{G}_{N+2\nu} \in \mathbb{R}^{(N+2\nu)\times(N+2\nu)}$ represents the Toeplitz matrix whose first row and first column are given by $[g(0), g(-T), \cdots, g(-(N+2\nu)T)]$ and $[g(0), g(T), \cdots, g((N+2\nu)T)]^T$, respectively. Moreover, ϕ_k represents the kth diagonal element of $\mathbf{\Phi}$,[1] and $\mathrm{tr}\{\cdot\}$ represents the trace operation. If the precoding matrix be $\mathbf{P} = \mathbf{I}_N$, the average transmit energy is given by [14]

$$E = N\sigma_{\mathrm{s}}^2. \tag{44}$$

To maintain the transmit energy per block to be unchanged regardless of $\mathbf{P}$, the energy constraint of $E = N\sigma_{\mathrm{s}}^2$ is imposed. With (44) and (42), we arrive at the energy constraint of

$$\sum_{k=0}^{N-1} \gamma_k \phi_k = N, \tag{45}$$

With (34) and (45), the Lagrange function is formulated by

$$J = \sum_{k=0}^{N-1} \log_2\left(1 + \frac{\sigma_{\mathrm{s}}^2}{N_0}\gamma_k \theta_k^2 \psi_k^{-1}\right) - \alpha\left(\sum_{k=0}^{N-1}\gamma_k\phi_k - N\right), \tag{46}$$

where α is the Lagrange multiplier. To maximize (46), the following problem is solved [12]:

$$\frac{\partial J}{\partial \gamma_k} = 0, \ \text{subject to } \gamma_k \geq 0. \tag{47}$$

Finally, the optimal coefficients γ_k are given by

$$\gamma_k = \max\left(\frac{1}{\alpha\phi_k \ln 2} - \frac{\psi_k N_0}{\theta_k^2 \sigma_s^2}, 0\right), \tag{48}$$

which is calculated in the same manner as the classic water-filling algorithm [14, 20].

C. Detection Algorithm

In this section, the detection algorithm of the proposed FFT-spread FTN signaling scheme is presented. Let us set the weight matrix at the receiver to $\mathbf{W} = \mathbf{Q}$, and then the approximated received block is rewritten by

$$\begin{aligned}
\mathbf{r}_{\mathrm{d}} &\simeq \mathbf{Q}\mathbf{G}_{\mathrm{c}}\mathbf{x} + \mathbf{Q}\boldsymbol{\eta} && (49)\\
&= \mathbf{Q}\mathbf{Q}^H\mathbf{\Theta}\mathbf{Q}\mathbf{Q}^H\mathbf{\Gamma}^{\frac{1}{2}}\mathbf{s} + \boldsymbol{\eta}_{\mathrm{q}} && (50)\\
&= \mathbf{\Theta}\mathbf{\Gamma}^{\frac{1}{2}}\mathbf{s} + \boldsymbol{\eta}_{\mathrm{q}}, && (51)
\end{aligned}$$

where $\boldsymbol{\eta}_{\mathrm{q}} = \mathbf{Q}\boldsymbol{\eta}$. The covariance matrix of the noise components $\boldsymbol{\eta}_{\mathrm{q}}$ is approximately calculated by

$$\begin{aligned}
\mathbb{E}[\boldsymbol{\eta}_{\mathrm{q}}\boldsymbol{\eta}_{\mathrm{q}}^H] &= \mathbf{Q}\mathbb{E}[\boldsymbol{\eta}\boldsymbol{\eta}^H]\mathbf{Q}^H && (52)\\
&= N_0\mathbf{Q}\mathbf{G}\mathbf{Q}^H && (53)\\
&\simeq N_0\mathbf{Q}\mathbf{Q}^H\mathbf{\Psi}\mathbf{Q}\mathbf{Q}^H && (54)\\
&= N_0\mathbf{\Psi}. && (55)
\end{aligned}$$

[1]Note that $\mathbf{\Phi}$ is calculated offline since the matrices $\mathbf{Q}$, $\mathbf{A}_{\mathrm{cp}}$, and $\mathbf{G}_{N+2\nu}$ do not include channel state information (CSI), hence known in advance of transmission.

As shown in (51) and (55), the received block and the noise correlation matrix are approximately diagonalized. This allows us to carry out efficient sub-optimal symbol-by-symbol demodulation while reducing the effects of the correlated noises.

In the proposed FFT-spread FTN signaling, the matrix $\mathbf{G}$ is approximated by $\mathbf{Q}^H\mathbf{\Psi}\mathbf{Q}$, where the approximation may cause the ill-conditioned problem for around the boundary of $\tau = 1/(1+\beta)$. Our extensive simulations revealed that for $\tau = 1/(1+\beta)$, the approximated eigenvalues may be negative, depending on m. To avoid this, in this paper, we impose further limitation on the packing ratio τ, i.e., $1/(1+\beta)+\delta \leq \tau \leq 1$, to ensure all the positive eigenvalues, where $\delta \in \mathbb{R}$ is a predefined small value. In our simulations, δ was set as 0.02.

In our proposed FFT-spread FTN signaling with optimal power allocation, the eigenvalues θ_k and ϕ_k are the FFT coefficients, while the multiplications of the precoding matrix $\mathbf{P} = \mathbf{Q}^H\mathbf{\Gamma}^{\frac{1}{2}}$ and the weighting matrix $\mathbf{W} = \mathbf{Q}$ are efficiently computed by the IFFT and FFT, respectively. Furthermore, the power allocation coefficients (48) are computed by the order of $\mathcal{O}(N)$. Thus, the computational complexity of the proposed FFT-spread FTN transceiver is given by $\mathcal{O}(N\log N)$.

III. Simulation Results

In this section, we provide the simulation results to investigate the BER performance of the proposed FFT-spread FTN signaling scheme. We considered the frequency-selective Rayleigh block fading channel with the L-tap, and the channel coefficients h_l were randomly generated according to the complex-valued Gaussian distribution of $\mathcal{CN}(0, 1/L)$. The basic system parameters of $N = 1024$ and $\beta = 0.25$ were set throughout the simulations.

In our BER calculations, we considered the three-stage serially-concatenated turbo coding architecture of [14], where the half-rate recursive systematic coding (RSC) encoder having the constraint length of 2 and octal generator polynomial $(3, 2)$ was employed as the outer encoder, while the unity rate coding encoder was used as the inner encoder [21]. The number of outer decoding iteration and that of inner decoding iteration were set to 40 and 2, respectively [14]. Moreover, the target interleaver length was set to around 200000 bits.[2] Similar to conventional EVD-precoded FTN signaling [14], the log-likelihood ratio (LLR) of the received symbols is efficiently calculated since the equivalent channel matrix and the noise covariance matrix are approximately diagonalized.

The transmission rate of the proposed half-rate turbo-encoded FFT-spread FTN signaling system is given by

$$R_{\mathrm{t}} = \frac{1}{2}\cdot\frac{1}{2W(1+\beta)}\cdot\frac{1}{(N+2\nu)\tau T_0}\cdot\sum_{k=0}^{N-1} b_k \ \text{[bps/Hz]}, \tag{56}$$

where the coefficient $1/2$ represents the coding rate of the RSC code, and b_k denotes the number of bits assigned onto

[2]Similar to [14], multiple transmit blocks having the N symbols were concatenated by ignoring the detrimental IBI effects for simplicity.

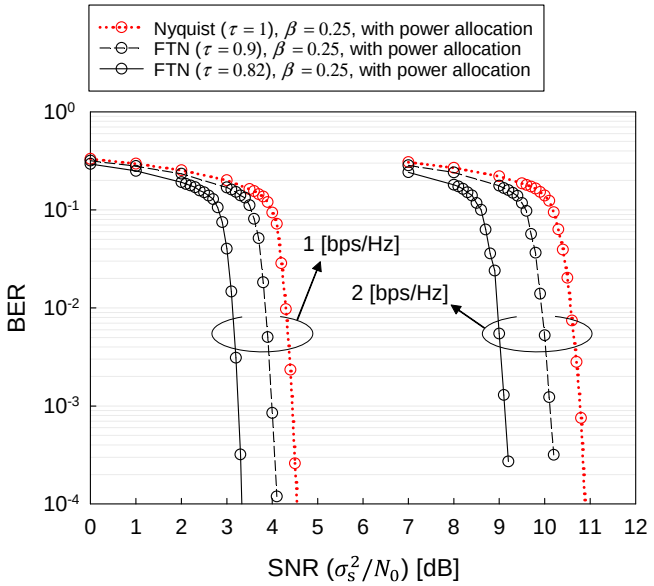

Fig. 2. BER performance of the proposed FTN signaling scheme with optimal power allocation. The roll-off factor was fixed to $\beta = 0.25$, while the packing ratio was given by $\tau = 0.9$ and 0.82. The other system parameters were set to $N = 1024$, $L = 20$, and $\nu = 30$, and the target transmission rate was set to $R_{\rm t} = 1$ and 2.

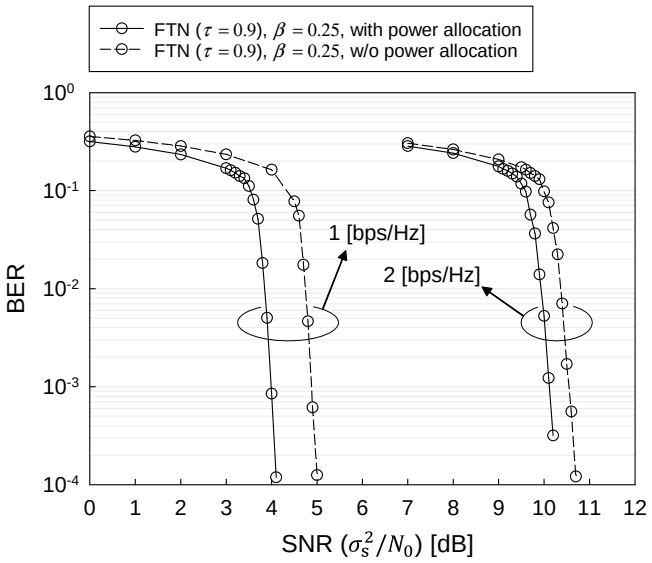

Fig. 3. BER performance of the proposed FTN signaling schemes with and without optimal power allocation. The system parameters were set to $\beta = 0.25$, $\tau = 0.9$, $N = 1024$, $L = 20$, and $\nu = 30$. The target transmission rate was set to $R_{\rm t} = 1$ and 2.

the kth symbol. The part of the symbols is deactivated when the associated power allocation coefficients were $\gamma_k = 0$ as an optimization result of (48). Hence, the number of bits b_k change depending on CSI to maintain the target transmission rate, which is referred to as *bit-loading* in this paper.[3]

Fig. 2 shows the BERs of the three-stage turbo-coded FFT-spread FTN signaling scheme with optimal power allocation, where the packing ratio was given by $\tau = 0.9$ and 0.82, and other system parameters were given by $L = 20$, and $\nu = 30$. The target transmission rate was set to $R_{\rm t} = 1$ and 2. For comparison, the BER curves of Nyquist signaling counterpart ($\tau = 1$) employing the same RRC shaping filter were plotted, where we set $2\nu = L = 20$ [22, 23]. Observe in Fig. 2 that the proposed scheme achieved better BER performance than its Nyquist signaling counterpart, and the proposed FTN scheme with $\tau = 0.82$ achieved the best BER performance. More specifically, upon increasing the target transmission rate from $R_{\rm t} = 1$ to 2, the performance advantage of the proposed scheme with $\tau = 0.82$ over the Nyquist signaling counterpart increased from 1.2 dB to 1.8 dB.

Fig. 3 shows the BERs of the proposed schemes with and without optimal power allocation. For the proposed scheme without power allocation, we set $\gamma_k = 1$ $(k = 0, \cdots, N-1)$ which dispenses with CSI for precoding, unlike the proposed scheme with power allocation. This implies that the proposed scheme without power allocation is the open-loop system, while the proposed scheme with power allocation is the closed-loop one. The packing ratio was set to $\tau = 0.9$, and other system parameters were the same as those used in Fig. 2. As shown in Fig. 3, our optimal power allocation allows us to have the better BER performance, where the gap decreased upon increasing the transmission rate. More specifically, the gaps were 0.9 dB and 0.4 dB for $R_{\rm t} = 1$ and 2, respectively.

Furthermore, Fig. 4 shows the BER comparisons between the proposed scheme with and without optimal power allocation, the EVD-precoded FTN signaling scheme with optimal power allocation [14], and the open-loop SoD-FDE-aided FTN signaling scheme with soft cancellation [10]. Note that the computational complexity in the proposed scheme is as low as $\mathcal{O}(N \log N)$, while those of the EVD-precoded FTN signaling scheme and the open-loop SoD-FDE-aided FTN signaling scheme with soft cancellation are $\mathcal{O}(N^3)$ and $\mathcal{O}(N^2)$, respectively. The system parameters were set to $\tau = 0.82$, $L = 20$, and $\nu = 30$. The target transmission rate was set to $R_{\rm t} = 0.461$ for each scheme. In Fig. 4, it was observed that the proposed scheme with optimal power allocation outperformed two other open-loop schemes, i.e., SoD-FDE-aided unprecoded FTN signaling scheme [10] and the proposed FTN scheme without power allocation, where the associated performance gaps were 2.1 dB and 3.2 dB, respectively. Naturally, the EVD-precoded FTN signaling with optimal power allocation [14] exhibited the best performance owing to the optimality in terms of an achievable information rate, which is achieved at the cost of prohibitively high computational complexity. The penalty of the proposed scheme with optimal power allocation over

[3]In our simulations, binary phase-shift keying (BPSK) was used for all the activated symbols. Then, quadrature PSK (QPSK) was used to replace the BPSK-modulated symbols from the first activated symbol to the last one until the target transmission rate was achieved. The same operation was repeated using 16-point quadrature amplitude modulation (QAM), 64-QAM, 256-QAM, and 1024-QAM until the target transmission rate was achieved.

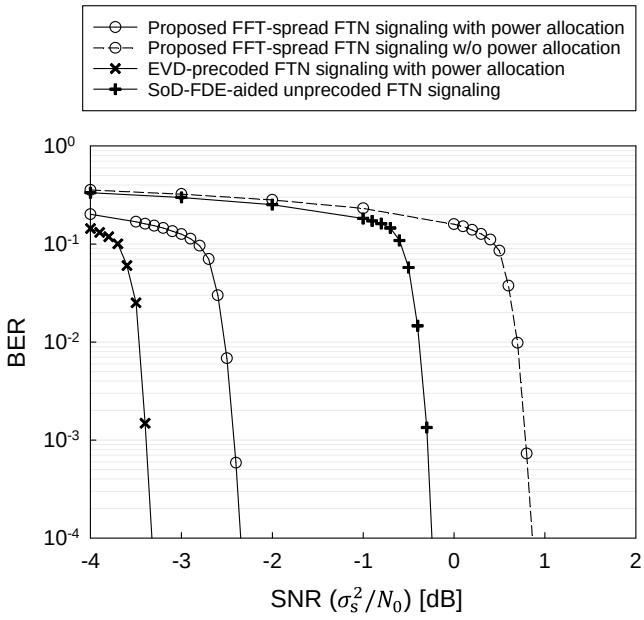

Fig. 4. BER comparisons between the proposed FTN signaling schemes with and without optimal power allocation, the EVD-precoded FTN signaling scheme with optimal power allocation [14], and the open-loop SoD-FDE-aided FTN signaling scheme with soft cancellation [10]. The system parameters were set to $\beta = 0.25$, $\tau = 0.82$, $N = 1024$, $L = 20$, $\nu = 30$, and $R_{\rm t} = 0.461$.

the EVD-precoded FTN signaling scheme with optimal power allocation [14] is imposed due to the circulant matrix approximation and the power penalty caused by the CP insertion. Note that a sufficiently long guard interval has to be added for the EVD-precoded FTN signaling benchmark [14] to eliminate the detrimental IBI effects, while it was ignored in our simulations.

IV. Conclusions

In this paper, we proposed the novel reduced-complexity FFT-spread FTN signaling with optimal power allocation for a frequency-selective fading channel. Under the circulant matrix approximation of the equivalent channel matrix and the noise covariance matrix, the approximated information rate of the proposed scheme was formulated. Then, the optimal power allocation coefficients were derived by maximizing the approximated information rate. Our simulation results demonstrated that the proposed FTN signaling scheme achieved the BER performance close to the EVD-precoded FTN signaling bound, which is optimal in terms of an information rate while reducing the transceiver's computational complexity imposed by the calculations of precoding and weighting matrices.

Acknowledgement

The work of T. Ishihara was supported in part by the Japan Society for the Promotion of Science (JSPS) KAKENHI (Grant Number 20K22410). The work of S. Sugiura was supported in part by the Japan Science and Technology Agency (JST) Precursory Research for Embryonic Science and Technology (PRESTO) (Grant Number JPMJPR1933).

References

[1] B. Saltzberg, "Intersymbol interference error bounds with application to ideal bandlimited signaling," *IEEE Transactions on Information Theory*, vol. 14, no. 4, pp. 563–568, July 1968.

[2] J. Anderson, F. Rusek, and V. Öwall, "Faster-than-Nyquist signaling," *Proceedings of the IEEE*, vol. 101, no. 8, pp. 1817–1830, Aug. 2013.

[3] T. Ishihara, S. Sugiura, and L. Hanzo, "The evolution of faster-than-Nyquist signaling," *IEEE Access*, vol. 9, pp. 86 535–86 564, June 2021.

[4] A. D. Liveris and C. N. Georghiades, "Exploiting faster-than-Nyquist signaling," *IEEE Transactions on Communications*, vol. 51, no. 9, pp. 1502–1511, Sep. 2003.

[5] A. Prlja, J. B. Anderson, and F. Rusek, "Receivers for faster-than-Nyquist signaling with and without turbo equalization," in *IEEE International Symposium on Information Theory*, July 2008, pp. 464–468.

[6] A. Prlja and J. B. Anderson, "Reduced-complexity receivers for strongly narrowband intersymbol interference introduced by faster-than-Nyquist signaling," *IEEE Transactions on Communications*, vol. 60, no. 9, pp. 2591–2601, Sep. 2012.

[7] S. Li, B. Bai, J. Zhou, P. Chen, and Z. Yu, "Reduced-complexity equalization for faster-than-Nyquist signaling: New methods based on Ungerboeck observation model," *IEEE Transactions on Communications*, vol. 66, no. 3, pp. 1190–1204, Mar. 2018.

[8] S. Sugiura, "Frequency-domain equalization of faster-than-Nyquist signaling," *IEEE Wireless Communications Letters*, vol. 2, no. 5, pp. 555–558, Oct. 2013.

[9] S. Sugiura and L. Hanzo, "Frequency-domain-equalization-aided iterative detection of faster-than-Nyquist signaling," *IEEE Transactions on Vehicular Technology*, vol. 64, no. 5, pp. 2122–2128, May 2015.

[10] T. Ishihara and S. Sugiura, "Iterative frequency-domain joint channel estimation and data detection of faster-than-Nyquist signaling," *IEEE Transactions on Wireless Communications*, vol. 16, no. 9, pp. 6221–6231, Sep. 2017.

[11] Y. J. D. Kim, "Properties of faster-than-Nyquist channel matrices and folded-spectrum, and their applications," in *IEEE Wireless Communications and Networking Conference*, Doha, Qatar, Apr. 2016, pp. 1–7.

[12] T. Ishihara and S. Sugiura, "SVD-precoded faster-than-Nyquist signaling with optimal and truncated power allocation," *IEEE Transactions on Wireless Communications*, vol. 18, no. 12, pp. 5909–5923, Dec. 2019.

[13] M. Mohammadkarimi, R. Schober, and V. W. S. Wong, "Channel coding rate for finite blocklength faster-than-Nyquist signaling," *IEEE Communications Letters*, vol. 25, no. 1, pp. 64–68, Jan. 2021.

[14] T. Ishihara and S. Sugiura, "Eigendecomposition-precoded faster-than-Nyquist signaling with optimal power allocation in frequency-selective fading channel," *IEEE Transactions on Wireless Communications*, 2021, in press.

[15] F. Rusek and J. B. Anderson, "Constrained capacities for faster-than-Nyquist signaling," *IEEE Transactions on Information Theory*, vol. 55, no. 2, pp. 764–775, Feb. 2009.

[16] T. Ishihara and S. Sugiura, "Comments on and corrections to "SVD-precoded faster-than-Nyquist signaling with optimal and truncated power allocation"," *TechRxiv*, pp. 1–1, 2021. [Online]. Available: https://doi.org/10.36227/techrxiv.14949681.v1

[17] T. M. Cover and J. A. Thomas, *Elements of Information Theory*. New York: Wiley, 1991.

[18] R. M. Gray, *Toeplitz and circulant matrices: A review*, department of Electrical Engineering, Stanford, Tech. Rep., 2006. [Online] Available: http://ee.stanford.edu/˜gray/toeplitz.pdf.

[19] A. Dembo, T. M. Cover, and J. A. Thomas, "Information theoretic inequalities," *IEEE Transactions on Information Theory*, vol. 37, no. 6, pp. 1501–1518, Nov. 1991.

[20] A. Goldsmith, *Wireless communications*. Cambridge University Press, 2005.

[21] D. Divsalar, S. Dolinar, and F. Pollara, "Serial concatenated trellis coded modulation with rate-1 inner code," in *IEEE Global Telecommunications Conference*, vol. 2, San Francisco, CA, Nov. 2000, pp. 777–782.

[22] N. Al-Dhahir, "Single-carrier frequency-domain equalization for space-time block-coded transmissions over frequency-selective fading channels," *IEEE Commun. Lett.*, vol. 5, no. 7, pp. 304–306, July 2001.

[23] D. Falconer, S. L. Ariyavisitakul, A. Benyamin-Seeyar, and B. Eidson, "Frequency domain equalization for single-carrier broadband wireless systems," *IEEE Commun. Mag.*, vol. 40, no. 4, pp. 58–66, Apr. 2002.